Surface flows of granular materials: A modified picture for thick avalanches

Thomas Boutreux, Elie Raphaël, and Pierre-Gilles de Gennes
Collège de France, 11 Place M. Berthelot, 75231 Paris Cedex 05, France
(Received 18 March 1998)

Some time ago, Bouchaud *et al.* [J. Phys. I **4**, 1383 (1994)] proposed a basic set of equations to describe surface flows. They assumed in particular that the rate of erosion (or accretion, depending on the slope) was proportional to the local amount R of rolling species. This is natural for thin avalanches, but not for thick avalanches. We discuss here the thick limit and assume that for $R \gg d$ (the grain diameter) the rates become independent of R. This leads to some different features: (i) filling of a silo, for which the steady-state slope is a (decreasing) function of the feeding rate; (ii) avalanches with a sink at the bottom end (''open cells''), for which the profile starts at a certain angle $\theta_{\max}$ and ends at the neutral angle θ_n, where θ_n is the angle at which erosion balances accretion and is smaller than $\theta_{\max}$ ($\theta_n = \theta_{\max} - \delta$); and (iii) avalanches with a closed end (where the flow stops), for which the angle of repose is *not* θ_n but $\theta_n - \delta = \theta_{\max} - 2\delta$. Each avalanche involves a cascade of successive regimes that are described analytically. [S1063-651X(98)03910-5]

PACS number(s): 83.10.Hh

I. GENERAL PRINCIPLES

A. Onset of avalanches

When constructing Fort Bourbon, Coulomb (who was at the time a military engineer) noticed that a granular system, with a slope angle θ larger than a critical value $\theta_{\max}$, would be unstable. He related the angle $\theta_{\max}$ to the friction properties of the material. For granular materials, with negligible adhesive forces, the simple argument of Fig. 1 leads to $\tan \theta_{\max} = \mu$, where μ is a friction coefficient [1]. The instability generates an avalanche. Our aim, in the present paper, is to propose a detailed scenario for the avalanche.

We note first that the Coulomb argument is not complete: (a) It does not tell us at what angle $\theta_{\max} + \varepsilon$ the process will actually start and (b) it does not tell us which gliding plane is preferred (among those of angle $\theta_{\max}$) as shown in Fig. 1. We shall propose an answer to these questions based on the notion of a characteristic mesh size ξ in the granular material.

Simulations [2,3] and experiments [4] indicate that the forces are not uniform in a granular medium, but that there are force paths conveying a large fraction of the force. These paths have a certain mesh size ξ that is dependent of the grain shapes, the friction forces between them, etc., but is typically $\xi \sim 5-10$ grain diameter d.

We also know that, under strong shear, a granular material can display *slip bands* [5]. The detailed geometry of these bands depends on the imposed boundary conditions. However, the minimum size of a slip band appears to be larger than d. We postulate that the minimum size *coincides with the mesh size* ξ.

We are then able to make a plausible prediction for the onset of the Coulomb process: The thickness of the excess layer must be of order ξ and the excess angle ε must be of order ξ/L, where L is the size of the free surface. Thus, at the moment of onset, our picture is that a layer of thickness $\sim \xi$ starts to slip. It shall then undergo various processes: (i) It shall be fluidized by the collisions on the underlying heap and (ii) it shall be amplified because the rolling grains destabilize some other grains below. The steady-state flow has been studied in detailed simulations [6]. It shows a sharp boundary between rolling grains and immobile grains: This is the starting point of sharp boundary between rolling grains and immobile grains and the starting point of most current theories.

The amplification process was considered in some detail by Bouchaud, Cates, Ravi Prakash, and Edwards (BCRE) in a classic paper of 1994 [7,8]. It is important to realize that, if we start with a thickness ξ of rolling species, we rapidly reach much larger thicknesses R. In practice, with macroscopic samples, we deal with *thick avalanches* ($R \gg \xi$). We are mainly interested in these regimes, which will in fact turn out to be relatively simple.

B. BCRE's modified equations

BCRE discuss surface flows on a pile of profile $h(x,t)$ and local slope $\tan \theta \cong \theta = \partial h / \partial x$, with a certain amount $R(x,t)$ of rolling species (Fig. 2). In Ref. [7] the evolution equation for the profile $h(x,t)$ is written in the form

$$\frac{\partial h}{\partial t} = \gamma R(\theta_n - \theta) + (\text{diffusion terms}), \tag{1}$$

where γ is a characteristic frequency and the angle θ_n is a constant. This gives erosion for $\theta > \theta_n$ and accretion for $\theta < \theta_n$. We call θ_n the neutral angle. This notation differs from that of BCPE, who called the constant angle appearing in Eq. (1) θ_r, the angle of repose. Our point is that different

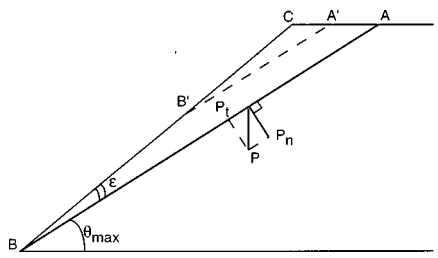

FIG. 1. Coulomb method of wedges to define the angle $\theta_{\max}$ at which an avalanche starts.

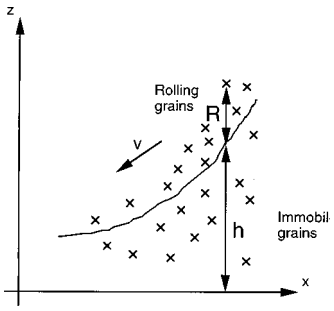

FIG. 2. The basic assumption of the BCRE picture is that there is a sharp distinction between immobile grains with a profile $h(x,t)$ and rolling grains of thickness $R(x,t)$. R is measured in units of ''equivalent height'': collision processes conserve the sum $h+R$.

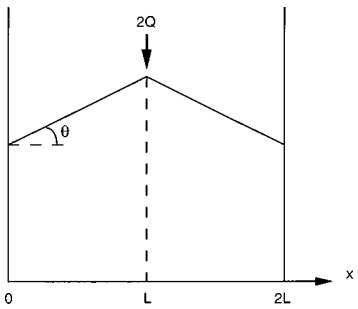

FIG. 3. Steady-state feeding of a two-dimensional silo with a flux $2Q$ over a length $2L$, leading to a constant growth velocity Q/L.

experiments can lead to different angles of repose, i.e., to different final slopes of the pile at the end of the avalanche, not always equal to θ_n.

For the rolling species, BCRE write

$$\frac{\partial R}{\partial t} = -\frac{\partial h}{\partial t} + v\,\frac{\partial R}{\partial x} + (\text{diffusion terms}), \tag{2}$$

where v is a flow velocity, assumed to be nonvanishing (and approximately constant) for $\theta \sim \theta_n$. For simple grain shapes (spheroidal) and average levels of inelastic collisions, we expect $v \sim \gamma d \sim (gd)^{1/2}$, where d is the grain diameter and g the gravitational acceleration. Equation (1) gives $\partial h/\partial t$ as linear in R: This should hold at small R, when the rolling grains act independently, but when $R > \xi$, this is not acceptable. The grains in the upper part of the rolling phase cannot interact any longer with the static phase since they are screened off by particles in the lower part of the rolling phase. Consider, for instance, the ''uphill waves'' mentioned by BCRE, where R is constant: Eq. (1) shows that an accident in slope moves upward, with a velocity $v_{\rm up} = \gamma R$. It is not natural to assume that $v_{\rm up}$ can become very large for large R.

This leads us to propose a modified version of BCRE's equation valid for flows that involve large R values and of the form

$$\frac{\partial h}{\partial t} = v_{\rm up}(\theta_n - \theta) \quad (R > \xi), \tag{3}$$

where $v_{\rm up}$ is a constant, comparable to v. Our aim here is to show the consequences of this modification.

Remark. In the present problems, the diffusion terms in Eq. (2) turn out to be small when compared to the convective terms (of order d/L, where L is the size of the sample): we omit them systematically.

C. A simple case

A first basic example (Fig. 3) is a two-dimensional silo, fed from a point at the top, with a rate $2Q$, and extending over a horizontal span $2L$: The height profile moves upward with a constant velocity Q/L. The profiles (which are symmetrical around $x = L$) were already analyzed within the BCRE equations [9]. With the modified version, the R profile stays the same, vanishing at the walls:

$$R = \frac{x}{L}\,\frac{Q}{v} \quad (0 < x < L), \tag{4}$$

but the angle θ is modified and *differs from the neutral angle*; setting $\partial h/\partial t = Q/L$, we arrive at

$$\theta_n - \theta = \frac{Q}{L v_{\rm up}} \quad (0 < x < L). \tag{5}$$

Thus, using our modified version of BCRE's equation, which should be valid here for $Q > v\xi$, we expect a slope that is now dependent on the rate of filling: This might be tested in experiments or in simulations.

II. DOWNHILL AND UPHILL MOTIONS

Our starting point is a supercritical slope, extending over a horizontal span L with an angle $\theta = \theta_{\max} + \varepsilon$ (Fig. 1). Following the ideas of Sec. I, the excess angle ε is taken to be small (of order ξ/L). It will turn out that the exact value of ε is not important: As soon as the avalanche starts, the population of rolling species grows rapidly and becomes independent of ε (for ε small). This means that our scenarios have a certain level of universality. The crucial feature is that grains roll down, but profiles move uphill. We shall explain this in detail in the following subsection.

A. Wave equations and boundary conditions

It is convenient to introduce a reduced profile

$$\tilde{h}(x,t) = h(x,t) - \theta_n x_n. \tag{6}$$

Following BCRE, we constantly assume that the angles θ are not very large and write $\tan\theta \sim \theta$: This simplifies the notation. Ultimately we may write Eqs. (2) and (3) in the compact form

$$\frac{\partial R}{\partial t} = -\frac{\partial \tilde{h}}{\partial t} + v\,\frac{\partial R}{\partial x}, \tag{7}$$

$$\frac{\partial \tilde{h}}{\partial t} = -v_{\rm up}\,\frac{\partial \tilde{h}}{\partial x}. \tag{8}$$

Another important condition is that we must have $R > 0$. If we reach $R = 0$ in a certain interval of x, we must then replace Eq. (8) by

$$\frac{\partial \tilde{h}}{\partial t}=0. \tag{9}$$

One central feature of the modified equations (7) and (8) is that, whenever $R>0$, they are *linear*. The reduced profile $\tilde{h}$ is decoupled from R and follows a very simple wave equation

$$\tilde{h}(x,t)=w(x-v_{\mathrm{up}}t), \tag{10}$$

where w is an arbitrary function describing uphill waves.

It is also possible to find a linear combination of $R(x,t)$ and $\tilde{h}(x,t)$ that moves downhill. Let us set

$$R(x,t)+\lambda\tilde{h}(x,t)=u(x,t), \tag{11}$$

where λ is an unknown constant. Inserting Eq. (11) into Eq. (7), we arrive at

$$\frac{\partial u}{\partial t}-v\,\frac{\partial u}{\partial x}=[v_{\mathrm{up}}-\lambda(v_{\mathrm{up}}+v)]\,\frac{\partial \tilde{h}}{\partial x}. \tag{12}$$

Thus, if we choose

$$\lambda=\frac{v_{\mathrm{up}}}{v+v_{\mathrm{up}}}, \tag{13}$$

we find that u is ruled by a simple wave equation and we may set

$$u(x,t)=u(x+vt). \tag{14}$$

We can rewrite Eq. (11) in the form

$$R(x,t)=u(x+vt)-\lambda w(x-v_{\mathrm{up}}t). \tag{15}$$

Equations (10) and (15) represent the formal solution of our problem in all regions where $R>0$. We shall see that this formal solution leads in fact to a great variety of avalanche regimes.

B. Comparison of uphill and downhill velocities

Our equations introduce two velocities: one downhill (v) and one uphill (v_{up}). How are they related? The answer clearly depends on the precise shape (and surface features) of the grains. Again, if we go to spheroidal grains and average levels of inelasticity, we may try to relate v_{up} and v by a naive scaling argument. Returning to Eqs. (1) and (3) for the rate of exchange between fixed and rolling species, we may interpolate between the two limits ($R<\xi$ and $R>\xi$):

$$\frac{\partial h}{\partial t}=\gamma\xi f\left(\frac{R}{\xi}\right)(\theta_n-\theta), \tag{16}$$

where the unknown function f has the limiting behaviors

$$f(x\to 0)=x,\qquad f(x\gg 1)=f_\infty=\mathrm{const.} \tag{17}$$

This corresponds to $v_{\mathrm{up}}=f_\infty\gamma\xi$. Since we have assumed $v\sim\gamma d$, we are led to

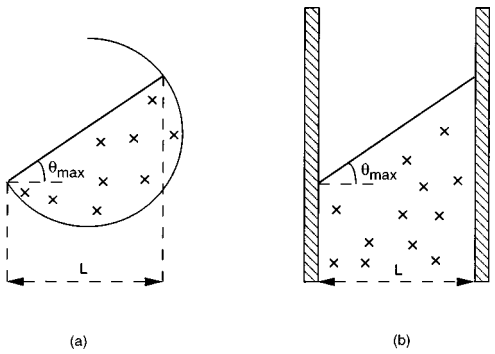

(a) (b)

FIG. 4. Two types of cells for avalanches: (a) open cell, with $h=$ const at the bottom of the slope, and (b) closed cell, with $R=0$ at the bottom.

$$v_{\mathrm{up}}/v\sim f_\infty\xi/d. \tag{18}$$

If, even more boldly, we assume that $f_\infty\sim 1$, since ξ is somewhat larger than the grain size, we are led to suspect that v_{up} may be larger than v. However, this is very tentative and in the following discussion we shall retain both possibilities $v_{\mathrm{up}}>v$ and $v_{\mathrm{up}}<v$. As we shall see, they lead to somewhat different scenarios.

C. Closed versus open systems

Various types of boundary conditions can be found for our problems of avalanches.

(a) At the top of the heap, we will consider situations of zero feeding ($R=0$). However, we could also have a constant injection rate Q fixing $R=Q/v$. This occurs in the silo of Fig. 3. It also occurs at the top of a dune under a steady wind, where saltation takes place on the windward side [10], imposing a certain injection rate Q, which then induces a steady-state flow on the steeper, leeward side.

(b) At the bottom end, we sometimes face a solid wall, e.g., in the silo; then we talk about a *closed* cell and impose $R=0$ at the left wall. However, in certain experiments, with a rotating bucket, the bottom end is *open* (Fig. 4). Here the natural boundary condition is $h=$ const at the bottom point and R is not fixed.

We discuss open cells in Sec. III and closed cells in Sec. IV. Within our model, the final states for these two types turn out to be deeply different.

III. THICK AVALANCHES IN AN OPEN SYSTEM

A. Onset

Our initial situation is shown in Fig. 4(a). As explained in Sec. I, at the starting time ($t=0$) we do have some rolling grains, but their number is few. We may thus use Eqs. (7) and (8) and the initial condition

$$R(x,t=0)=0. \tag{19}$$

Similarly (taking the origin of the x axis at the bottom point), we know the initial value of $\tilde{h}$

$$\tilde{h}(x,t=0)=(\theta_{\max}-\theta_n)x\equiv\delta x, \tag{20}$$

TABLE I. Avalanche in an open cell: summary of the different expressions for the amount R of rolling species and for the reduced profile $\tilde{h}$ of the static phase.

Act	Parameter	Bottom part	Central part	Top part
I	x	$0 \quad v_{\mathrm{up}}t$		$L-vt \quad L$
	R	$\lambda\delta(x+vt)$	$\delta v_{\mathrm{up}}t$	$\delta\frac{v_{\mathrm{up}}}{v}(L-x)$
	$\tilde{h}$	0	$\delta(x-v_{\mathrm{up}}t)$	$\delta(x-v_{\mathrm{up}}t)$
II	x	$0 \quad L-vt$		$v_{\mathrm{up}}t \quad L$
	R	$\lambda\delta(x+vt)$	$\lambda\delta\left(L-v_{\mathrm{up}}t+\frac{v_{\mathrm{up}}}{v}(L-x)\right)$	$\delta\frac{v_{\mathrm{up}}}{v}(L-x)$
	$\tilde{h}$	0	0	$\delta(x-v_{\mathrm{up}}t)$
III	x	$0 \quad L-vt$		$L-v\left(t-\frac{L}{v_{\mathrm{up}}}\right) \quad L$
	R	$\lambda\delta(x+vt)$	$\lambda\delta\left(L-v_{\mathrm{up}}t+\frac{v_{\mathrm{up}}}{v}(L-x)\right)$	0
	$\tilde{h}$	0	0	0

where δ is the (positive) difference between the maximum angle and the neutral angle.

B. Act I

During this act, we shall see that the amount of rolling species R grows in the container and that the profile $\tilde{h}$ starts to evolve. We express the solutions in terms of the two wave functions $w(z)$ (defined for $-\infty<z<L$) and $u(z)$ (defined for $0<z<+\infty$) introduced in Eqs. (10) and (15). Equation (20) imposes the values of w for $0<z<L$:

$$w(z)=\delta z \quad (0<z<L). \tag{21}$$

For an open system, the boundary condition is written

$$\tilde{h}(0,t)=h(0,t)=0. \tag{22}$$

This fixes w for negative arguments:

$$w(z)=0 \quad (z<0). \tag{23}$$

Let us now turn to the wave function $u(z)$. Equation (19) gives us a portion of it:

$$u(z)=\lambda\delta z \quad (0<z<L). \tag{24}$$

In concrete terms, we may describe the situation as follows. (i) We have an uphill wave [corresponding to the point $z=0$ of the function $w(z)$], starting at $t=0$ from the bottom end and reaching a point $x_u(t)=v_{\mathrm{up}}t$ at time t. (ii) We have a downhill wave [corresponding to the point $z=L$ of the function $u(z)$], starting from the top with velocity v and reaching the point $x_d(t)=L-vt$ at time t. We shall call act I the time interval $(0<t<\tau_l)$ where $x_u<x_d$, i.e., when the two fronts have not met.

During this act, we have three spatial regions in our avalanche: a bottom part $(0<x<x_u)$, a central part $(x_u<x<x_d)$, and a top part $(L>x>x_d)$. The solution given by Eqs. (21) and (24) gives us an answer only for the bottom and central parts. We can determinate $u(z)$ for $z>L$ (corresponding to the top part) by imposing the zero feeding boundary condition at the top:

$$R(x=L,t)=0. \tag{25}$$

Inserting this into Eq. (15), we arrive at

$$\lambda w(L-v_{\mathrm{up}}t)=u(L+vt), \tag{26}$$

i.e.,

$$u(z)=\lambda w\left[L\left(1+\frac{v_{\mathrm{up}}}{v}\right)-z\,\frac{v_{\mathrm{up}}}{v}\right]. \tag{27}$$

While in Eq. (27) the argument of w satisfies $0<z<L$, we may use Eq. (21) for w, obtaining

$$u(z)=\lambda\delta\left[L\left(1+\frac{v_{\mathrm{up}}}{v}\right)-z\,\frac{v_{\mathrm{up}}}{v}\right] \quad \left[L<z<\left(1+\frac{v_{\mathrm{up}}}{v}\right)L\right]. \tag{28}$$

(Note that this is *not* a Dirac delta function, but a simple product.) We can now discuss the whole structure that is predicted for act I. Our results for an avalanche in an open cell are summarized in Table I.

1. The bottom part

Here Eq. (23) tells us that $\tilde{h}=0$ (i.e., the slope θ has already relaxed and is equal to the neutral angle θ_n) and thus $R=u(x+vt)$. We may use Eq. (24) for u and arrive at

$$R=\lambda\delta(x+vt) \quad (x<v_{\mathrm{up}}t). \tag{29}$$

In particular at the bottom of the slope $(x=0)$, R is finite. Some rolling grains fall out of the container with a flux that increases linearly in time.

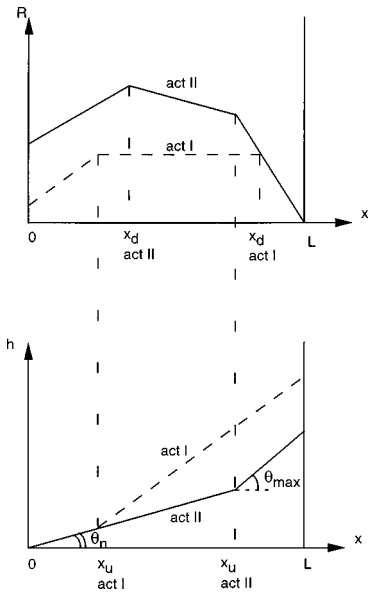

FIG. 5. Open cell act I (dashed lines) and act II (solid lines). An uphill wave starting from the bottom ($x=0$) has reached the point $x_u(t)=v_{up}t$. A downhill wave starting from the top has reached the point $x_d(t)=L-vt$. During act I the two fronts have not met ($x_u<x_d$); during act II they have passed each other.

2. The central part

Here Eq. (21) tells us that

$$\tilde{h}=\delta(x-v_{up}t) \quad (v_{up}t<x<L-vt). \tag{30}$$

The slope has not yet changed in this part of the container. Then Eqs. (15) and (24) give us

$$R=u(x+vt)-\lambda\tilde{h}=\delta v_{up}t \quad (v_{up}t<x<L-vt). \tag{31}$$

Thus, in the central part, the density of rolling species is independent of x and increases linearly in time.

3. The top part

Here we still use Eq. (30) for $\tilde{h}$, but we must now turn to Eq. (28) for $u(z)$. The result is

$$R=\delta\frac{v_{up}}{v}(L-x) \quad (L-vt<x<L). \tag{32}$$

The above expression is independent of time and vanishes at the uphill border ($x=L$). The structure of these profiles is shown in Fig. 5. Act I corresponds to the amplification of the avalanche via a large increase of the amount R of rolling grains. The maximum value of R, $R_{max}=\lambda\delta L$, is obtained at the end of act I, in the central region ($x=x_u=x_d$ at $t=\tau_l$).

C. Act II

The uphill front and the downhill front meet at a time

$$\tau_1=\frac{L}{v+v_{up}}. \tag{33}$$

At time $t>\tau_l$ they pass each other without any emission of secondary waves (since our equations are linear). Thus our solutions $u(z)$ and $w(z)$ remain valid. However, the spatial domains are different: The top region is bounded by

$$v_{up}t<x<L,$$

while the bottom region is defined by

$$x<L-vt$$

and the central region by

$$L-vt<x<v_{up}t.$$

The profile $\tilde{h}(x,t)$ retains its structure derived from Eqs. (10), (21), and (23): $\tilde{h}$ vanishes in the bottom and central regions and increases linearly (with slope δ) in the top region. In the bottom region, R is still given by Eq. (29) and in the top region by Eq. (32), as shown in Table I. In the central region, R is a linear interpolation between the values at x_u and x_d (Fig. 5), namely,

$$R=\lambda\delta\left(L-v_{up}t+\frac{v_{up}}{v}(L-x)\right). \tag{34}$$

In the bottom and central regions where $\tilde{h}=0$, there is no longer an amplification of the rolling grains. R is then simply convected downward at the constant speed v. $R_{max}=\lambda\delta L$ is now located at the point x_d.

D. Act III

The end of act II occurs when the uphill wave front reaches the border $x=L$ at the top of the container. Then act III begins at a time

$$\tau_{up}\equiv\frac{L}{v_{up}}. \tag{35}$$

At this time, the solution (34) for R vanishes at $x=L$. For $t>\tau_{up}$, it vanishes at a certain end point $x_s(t)$:

$$x_s=L-v\left(t-\frac{L}{v_{up}}\right). \tag{36}$$

The end point x_s sweeps from top to bottom during act III and reaches the bottom of the container ($x=0$) at the end time τ_e, defined by

$$\tau_e=\frac{L}{v}+\frac{L}{v_{up}}>\tau_{up}. \tag{37}$$

In the region $x<x_s$, the preceding solution of act II holds: $\tilde{h}\equiv 0$ and the rolling particles are convected downward. Note that at the beginning of act III, if $v<v_{up}$, the point $x_d(t)=L-vt$ (where the slope of R changes) is still located inside the container, close to its bottom end (as it appears in Fig. 6).

What happens for $x>x_s$? Our discussion in Sec. II tells us that for $x_s<x<L$ the system is *frozen* with $R=0$ and $\partial\tilde{h}/\partial t=0$. Thus $\tilde{h}$ retains its previous value $\tilde{h}=0$ everywhere. During act III the slope corresponds to the neutral angle everywhere, but we still have some rolling species at $x<x_s(t)$, which are simply convected downward at speed v. All the rolling grains fall out of the cell when they reach the

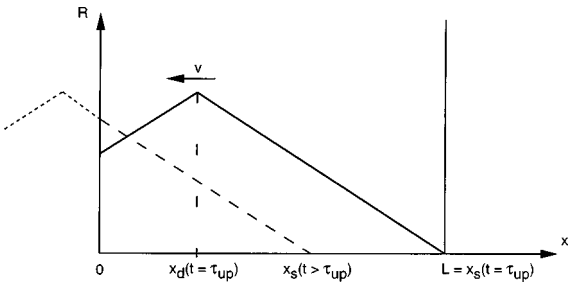

FIG. 6. Open cell act III. The rolling grains at $0<x<x_s(t)$ are simply convected downward. A frozen interval appears near the top $[x_s(t)<x<L]$. The case displayed here corresponds to $v_{up}>v$. At the beginning of act III, the point x_d is still inside the container.

border $x=0$. The successive aspects of $R(x,t)$ during act III are shown in Fig. 6, drawn for $v<v_{up}$. At $t=\tau_e$, there are no rolling grains left in the cell and the avalanche process ends. In this open cell, the angle of repose is therefore equal to the neutral angle θ_n.

IV. THICK AVALANCHES IN A CLOSED CELL

Here the starting point $(t=0)$ corresponds to a critical heap $(\theta=\theta_{max})$ between two walls, separated by a distance L. The initial conditions are the same; the only difference lies in the boundary condition at $x=0$, which now reads

$$R(0,t)=0. \tag{38}$$

This condition corresponds to a wall that prevents the rolling grains from leaving the container. The initial conditions fix the same structure for our wave functions $u(z)$ for $0<z<L$ [Eq. (24)] and $w(z)$ for $0<z<L$ [Eq. (21)]. The boundary condition at the top is unchanged and again gives us $u(z)$ for $L<z<L(1+v/v_{up})$ [Eq. (28)]. The main difference from Sec. III lies in the function $w(z)$ for $z<0$. When the boundary condition at the bottom [Eq. (38)] is inserted into Eq. (15), we get

$$w(-v_{up}t)=\delta v t,$$

$$w(z)=-\delta\frac{v}{v_{up}}z \quad \left(-\frac{v_{up}}{v}L<z<0\right). \tag{39}$$

A. Act I $[0<t<L/(v+v_{up})]$

Act I corresponds again to the amplification of the avalanche. The results are shown in Fig. 7 and are summarized in Table II.

1. The bottom part $(x<x_u\equiv v_{up}t)$

Here we have

$$\tilde{h}=\delta\frac{v}{v_{up}}(v_{up}t-x), \tag{40}$$

$$R=\delta x. \tag{41}$$

We have $\partial\tilde{h}/\partial x<0$: The slope is now smaller than the neutral angle θ_n. Hence the bottom part corresponds to a region of accretion of the rolling grains due to the wall located at

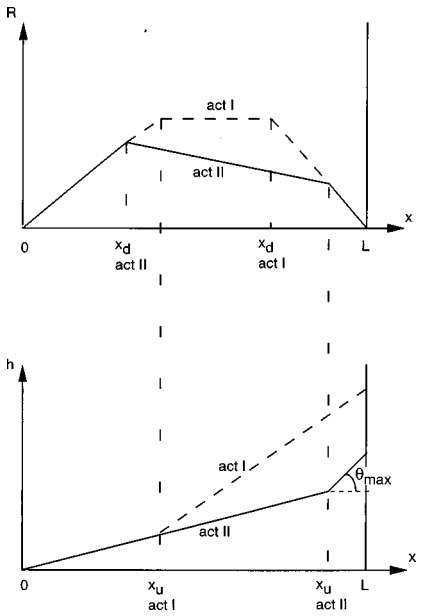

FIG. 7. Closed cell act I (dashed lines) and act II (solid lines). At the left of the uphill wave $[x<x_u(t)]$ the slope is smaller than θ_n [see Eq. (40)]. During act II the profile of R is drawn for $v_{up}>v$ (when $v_{up}<v$, $\partial R/\partial x$ in the central region becomes positive).

$x=0$. Note that such a region never appears during an avalanche in an open cell (Sec. III).

2. Central and top parts

The presence of the bottom wall does not yet affect inside the central part $(v_{up}t<x<L-vt)$ and the top part $(L-vt<x<L)$. Hence, for these parts, R and $\tilde{h}$ are the same as in the case of an open system; they are given in Table II.

B. Act II $[t>L/(v+v_{up})]$

The structure of u and w is the same as during act I, but the order of points (x_d,x_u) is altered. The results appear in Fig. 7. The explicit form of R in the central part is

$$R=\delta\left[x\left(1-\frac{v_{up}}{v}\right)-v_{up}t+\frac{v_{up}}{v}L\right]. \tag{42}$$

Note that $\partial R/\partial t$ is negative in this central region, which is a region of accretion since $\theta<\theta_n$. The sign of $\partial R/\partial x$ depends on the ratio v_{up}/v.

C. Act III

The end of act II occurs when the fastest wave front hits the opposite wall. If $v_{up}>v$, this occurs at the top; if $v_{up}<v$, this occurs at the bottom. Thus we must distinguish two cases (see Table II for the different expressions of R and $\tilde{h}$).

1. $v_{up}>v$

Act III begins at $t=\tau_{up}=L/v_{up}$ (see Fig. 8). Here we find again a frozen region starting from the top, in an interval $\tilde{x}_s(t)<x<L$:

$$\tilde{x}_s(t)=\frac{v_{up}}{v_{up}-v}(L-vt). \tag{43}$$

TABLE II. Avalanche in a closed cell: different expressions of R and $\tilde{h}$. Note that two different cases ($v_{up}>v$ or $v_{up}<v$) are possible during act III.

Act	Parameter	Bottom part		Central part		Top part
I	x	0	$v_{up}t$		$L-vt$	L
	R	δx		$\delta v_{up}t$		
				$\delta\frac{v_{up}}{v}(L-x)$		
	$\tilde{h}$	$\delta\frac{v}{v_{up}}(v_{up}t-x)$		$\delta(x-v_{up}t)$		$\delta(x-v_{up}t)$
II	x	0	$L-vt$		$v_{up}t$	L
	R	δx		$\delta\left[x\left(1-\frac{v_{up}}{v}\right)-v_{up}t+\frac{v_{up}}{v}L\right]$		$\delta\frac{v_{up}}{v}(L-x)$
	$\tilde{h}$	$\delta\frac{v}{v_{up}}(v_{up}t-x)$		$\delta\frac{v}{v_{up}}(v_{up}t-x)$		$\delta(x-v_{up}t)$
III ($v_{up}>v$)	x	0	$L-vt$		$\frac{v_{up}}{v_{up}-v}(L-vt)$	L
	R	δx		$\delta\left[x\left(1-\frac{v_{up}}{v}\right)-v_{up}t+\frac{v_{up}}{v}L\right]$		0
	$\tilde{h}$	$\delta\frac{v}{v_{up}}(v_{up}t-x)$		$\delta\frac{v}{v_{up}}(v_{up}t-x)$		$\delta(L-x)$
III ($v_{up}<v$)	x	0	$\frac{v_{up}}{v_{up}-v}(L-vt)$		$v_{up}t$	L
	R	0		$\delta\left[x\left(1-\frac{v_{up}}{v}\right)-v_{up}t+\frac{v_{up}}{v}L\right]$		$\delta\frac{v_{up}}{v}(L-x)$
	$\tilde{h}$	$\delta(L-x)$		$\delta\frac{v}{v_{up}}(v_{up}t-x)$		$\delta(x-v_{up}t)$

When t runs from τ_{up} to $\tau_d=L/v$, x_s sweeps the whole slope from top to bottom. When $\tilde{x}_s(t)$ reaches a given point, the rolling amount R vanishes and the granular media freezes at this point. The end of the avalanche now takes place at $t=\tau_d$, when the last rolling grains stop at $x=0$.

The frozen value of $\tilde{h}$ is given by $\tilde{h}(x,\tilde{t}_s(x))$, where $\tilde{t}_s(x)$ is the inverse function of $\tilde{x}_s(t)$. Using Eq. (43), we get for the frozen value of $\tilde{h}$

$$\overline{h}_{froz}(x)=\delta(L-x). \tag{44}$$

Thus, contrary to the case of an open cell, the final angle θ_f is *not* the neutral angle, but is smaller:

$$\theta_f=\theta_n-\delta. \tag{45}$$

This small final angle is due to the wall at the bottom of the container ($x=0$): The rolling grains cannot fall out of the cell and must accumulate near the wall at the bottom of the slope, thus reducing its final slope.

2. The case $v_{up}<v$

When $v_{up}<v$, the end of act II occurs at a time $\tau_d=L/v$ and corresponds to the downhill front reaching the bottom end (see Fig. 9). Act III corresponds to the interval $\tau_d<t<\tau_{up}$; during this time, the system freezes *from the bottom*. The frozen region occupies the interval $0<x<\tilde{x}_s$, where $\tilde{x}_s$ is still given by Eq. (43). $\tilde{x}_s$ now sweeps the slope from bottom to top. Again, we find that the final slope is $\theta_n-\delta$.

V. DISCUSSION

A. Three simple checks

The experimental determination of the whole profiles $h(x,t)$ and $R(x,t)$ on an avalanche represents a rather complex task. However, certain simple checks could easily be performed.

(a) With an *open cell*, the loss of material measured by $R(0,t)$ is easily obtained, for instance, by capacitance measurement [11]. Our predictions for this loss are described in Fig. 10. $R(0,t)$ increases linearly up to a maximum $R_{max}=\lambda\delta L$ at $t=L/v$ and then decreases linearly, reaching 0 at the final time $\tau_e=L(1/v+1/v_{up})$. The integrated amount is

$$M\equiv\int R(0,t)dt=\frac{\delta L^2}{2v}. \tag{46}$$

Unfortunately, the attention in Ref. [11] was focused mainly on the reproducibility of M, but (apparently) the value of M and the shape of $R(0,t)$ were not analyzed in detail.

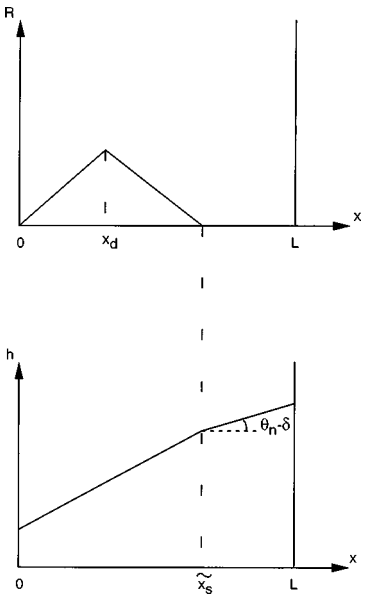

FIG. 8. Closed cell act III. The case $v_{up}>v$. A frozen patch, where the avalanche is terminated, grows from the top; in this patch, the final slope is $\theta_f=\theta_n-\delta$.

(b) With a *closed cell*, a simple observable is the rise of the height at the bottom $h(0,t)$. This is predicted to increase linearly with time,

$$h(0,t)=\tilde{h}(0,t)=\delta v t, \tag{47}$$

up to $t=L/v$, and to remain constant after. Similar measurements (both for open or closed cells) could be done at the top point, giving $h(L,t)$.

(c) A crucial parameter is the final angle θ_f. In our model, this angle is the same all along the slope. For an open cell, it is equal to the neutral angle θ_n. For a closed cell, it is *smaller*: $\theta_f=\theta_n-\delta=\theta_{max}-2\delta$.

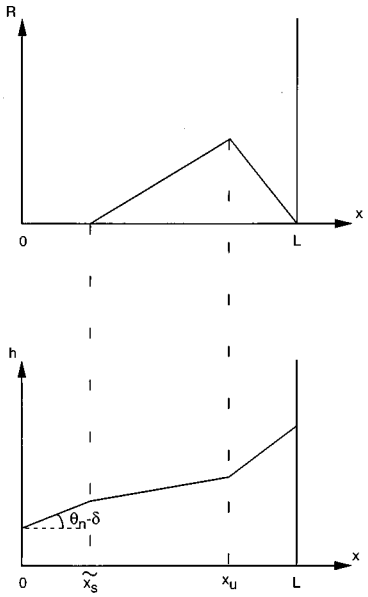

FIG. 9. Closed cell act III ($v_{up}<v$). Here a frozen patch grows *from the bottom*, where the final slope is again $\theta_f=\theta_n-\delta$.

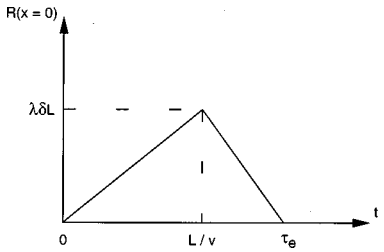

FIG. 10. Flux profile predicted at the bottom of an open cell. The maximum $R_{max}=\lambda\delta L$ is obtained for $t=L/v$.

Thus the notion of an angle of repose is not universal. The result for closed cell $\theta_f=\theta_n-\delta$ was already predicted in Ref. [12], where we proposed a qualitative discussion of thick avalanches. The dynamics (based on a simplified version of BCPE's equations) was unrealistic (too fast), but the conclusion on θ_f was obvious: In a closed cell, the material that starts at the top has to be stored at the bottom part and this leads to a decrease in slope.

Some recent experiments seem to indicate that indeed the angle of repose is not universal [13,14]. More experimental work will be needed, however, in order to check more precisely our predictions. For a detailed discussion, see the recent work of Boutreux [15].

(d) One major unknown of our discussion is the ratio v_{up}/v. We already pointed out that this may differ for different types of grains. Qualitative observations on a closed cell would be very useful here: If in its late stages (act III) the avalanche first freezes at the top, which means $v_{up}>v$. If it freezes from the bottom, $v_{up}<v$. If it does more complex things, this means that our model is wrong.

B. Limitation of the present model

1. Deterministic description

The avalanche starts automatically at $\theta=\theta_{max}+\varepsilon$ ($\approx\theta_{max}$ in the macroscopic limit) and sweeps the whole surface. In the open cell systems (with slowly rotating drums) one finds experimentally a nearly periodic set of avalanche spikes, suggesting that θ_{max} is well defined. However, the amplitude (and the duration) of these spikes varies [11]: It may be that some avalanches do not start from the top. We can only pretend to represent the full avalanches.

What is the reason for these statistical features? (i) Disparity in grain size tends to generate spatial inhomogeneities after a certain number of runs (in the simplest cases, the large grains roll further down and accumulate near the walls). (ii) Cohesive forces may be present: They tend to deform the final profiles, with a $\theta(x)$ that is not constant in space. (iii) Parameters such as θ_{max} (or θ_n) may depend on sample history.

2. Regions of small R

For instance, in a closed cell, $R(x,t)\to 0$ for $x\to 0$. A complete solution in the vicinity of $R=0$ requires more complex equations, interpolating between BCPE's and our linear set of equations, as sketched in Eq. (16). We have indeed investigated this point and found some solutions valid for all

R near a stopping wall. This shall be described elsewhere. It does not seem to alter significantly the macroscopic results described here.

3. Ambiguities in θ_n

When comparing thick and thin avalanches, we assumed that θ_n is the same for both; however, there may in fact be a small difference between the two. Since most practical situations are related to thick avalanches, we tend to focus our attention on the ''thick'' case, but this possible distinction between thick and thin should be kept in mind.

ACKNOWLEDGMENTS

We have greatly benefited from discussions and written exchanges with J. P. Bouchaud, J. Duran, P. Evesque, and J. Rajchenbach. We also thank N. Bloch for his indispensable help in drawing the figures.

[1] For a detailed description of the Coulomb approach and its extensions see R. Nedderman, *Statics and Kinematics of Granular Materials* (Cambridge University Press, Cambridge, 1992), in particular Chap. 4.

[2] F. Radjai, J.-J. Moreau, and S. Roux, Phys. Rev. Lett. **77**, 274 (1996).

[3] F. Radjai, D. Wolf, S. Roux, M. Jean, and J. J. Moreau, in *Powders and Grains*, edited by R. Behringer and J. Jenkins (Balkema, Rotterdam, 1997), p. 211.

[4] C. H. Liu, S. Nagel, D. Shechter, S. Coppermisth, S. Majumdar, O. Narayan, and T. Witten, Science **269**, 513 (1995).

[5] J. Desrues, in *Physics of Granular Media*, 1991 Les Houches Lectures, edited by D. Bideau and J. Dodds (Nova, Commack, NY, 1991).

[6] P. A. Thompson and G. S. Grest, Phys. Rev. Lett. **67**, 1751 (1991).

[7] J.-P. Bouchaud, M. Cates, Ravi Prakash, and S. F. Edwards, J. Phys. I **4**, 1383 (1994); J.-P. Bouchaud and M. Cates, in *Dry Granular Matter*, Proceedings of the Cargèse Workshop, 1997, edited by H. Hermann (unpublished).

[8] P.-G. de Gennes, *Powders and Grains* (Ref. [3]), p. 3.

[9] P.-G. de Gennes, C. R. Acad. Sci., Ser. IIb: Mec., Phys., Chim., Astron. **321**, 501 (1995).

[10] R. A. Bagnold, *The Physics of Blown Sand and Desert Dunes* (Chapman and Hall, London, 1984).

[11] H. Jaeger, C. Liu, and S. Nagel, Phys. Rev. Lett. **62**, 40 (1989).

[12] T. Boutreux and P. G. de Gennes, C. R. Acad. Sci., Ser. IIb: Mec., Phys., Chim., Astron. **325**, 85 (1997).

[13] P. Evesque and P. Poiron, in *Fragmentation Phenomena*, 1995 Les Houches Lectures, edited by D. Beysens *et al.* (Nova, Commack, NY, 1995).

[14] M. Caponeri, S. Douady, S. Fauve, and C. Laroche, in *Proceedings de l'Ecole d'été de Cargèse: Mobile Particulate Systems*, edited by E. Guazzelli and L. Oger (Kluwer, Amsterdam, 1995).

[15] T. Boutreux, Ph.D. thesis, Université Paris VI, 1998 (unpublished).